Metal and RNA Binding Properties of the hdm2 RING Finger Domain

Zhihong Lai,[‡] Deborah A. Freedman,[§] Arnold J. Levine,[§,||] and George L. McLendon*[,‡,§]

Departments of Chemistry and Molecular Biology, Princeton University, Princeton, New Jersey 08544

Received March 16, 1998; Revised Manuscript Received August 17, 1998

ABSTRACT: The hdm2 oncoprotein contains a C-terminal domain that binds RNA and has been suggested to bind zinc(II) in an unusual RING finger domain in which Thr 455 was postulated as a ligand. We have reported experiments to test whether this C-terminal cysteine-rich motif is indeed a RING finger domain. We also tested the affinity of the hdm2 C-terminal peptide for metal binding, metal linkage to the folding of the C-terminal peptide, and the peptide's affinity for RNA. Truncation mutants demonstrate that amino acids 425−491 are necessary and sufficient for RNA binding. However, divalent metal ions do not seem to affect the specific RNA recognition. Metal binding studies suggest that hdm2 indeed binds to two molecules of zinc in an intertwined motif similar to the BRCA1 RING finger peptide. However, there is no similarity in overall tertiary structure, nor is there direct sequence homology with other RING fingers. Fluorescence energy transfer studies give a dissociation constant of (0.22 ± 0.03) μM for cobalt(II) binding to site 1, while K_2 for cobalt(II) binding was estimated to be 15 ± 5 μM from ultraviolet absorbance. Studies of two mutant peptides confirm the assignment of binding residues in hdm2 and suggest that the coordination of Thr 455 previously proposed by sequence alignments is incorrect. Structural studies of hdm2 in the presence and absence of metal indicate only a small amount of secondary structure by circular dichroic spectroscopy. Metal binding did not seem to nucleate folding as in the case of two other RING finger proteins. However, distance measurement from fluorescence energy transfer indicated that the Tyr 489 residue was only ∼14 Å away from the first metal center, suggesting that the hdm2 protein exists in a compact form, at least in the presence of metal ion. In summary, hdm2 binds metal and RNA, but the RNA binding does not seem to occur in a zinc-dependent manner.

The RING finger motif is a conserved cysteine-rich amino acid sequence found in a variety of proteins (*1*−*3*). This motif has four pairs of metal binding residues with a characteristic linear sequence of Cys-X_2-Cys-$X_{(9-39)}$-Cys-$X_{(1-3)}$-His-$X_{(2-3)}$-Cys-X_2-Cys-$X_{(4-48)}$-Cys-X_2-Cys. X can be any amino acid, although some positions have a clear preference for certain type of residues. The RING finger (or C_3HC_4) domain binds to two zinc atoms per molecule in a cross-braced system, employing the first and third pairs of cysteines to form the first binding site and the second and fourth pairs of metal binding residues to form the other. Since this unique zinc binding motif was identified in the human *ring1* gene some six years ago, the number of family members has increased rapidly to nearly 80 now, with members found in animals, plants, and viruses. A common role of the RING finger domain remains unclear at the moment, although it was speculated that it may function as a protein−protein interaction domain or a nucleic acid binding domain. There are a number of RING finger proteins with oncogenic potential, including the protein encoded by the breast cancer susceptibility gene BRCA1 (*3*−*5*). Recently, another oncoprotein, hdm2 (human form of mdm2), was also postulated to contain the RING finger motif (*3, 6*). The RING finger domain from hdm2 is studied in this present work.

The hdm2 gene is overexpressed in a significant number of sarcomas, osteosarcomas, and gliomas (*7*−*11*). The hdm2 protein is believed to be oncogenic by binding to the tumor suppressor protein p53, thereby inactivating its function as a transcription factor (*10, 12, 13*). The N-terminal amino acid residues of the hdm2 protein interact with the N-terminal transactivation domain of the p53 protein and block p53's ability to transcriptionally activate gene expression (*14, 15*). The hdm2 protein also regulates the level of p53 by targeting it for degradation (*16, 17*). It has been shown that the hdm2 protein also interacts with other proteins that may also enhance its oncogenic potential. In addition to the N-terminal p53 binding domain, the hdm2 protein also contains a nuclear localization signal, a nuclear export signal, a central acidic domain, a C_4 zinc finger domain, and a C-terminal cysteine-rich motif, which was initially proposed to contain two tandem zinc fingers of the C_2H_2 and C_4 type (*10, 13, 18*). By sequence alignment, Boddy and Freemont (*6*) proposed that this motif of the hdm2 protein was a RING finger motif, implying that it would bind to two molecules of zinc in an interleaved fashion and fold into a single domain. They also proposed that Thr 455 of hdm2 was used to substitute for the third Cys in the sequence, leading to the formation of site 2 with His 457, Cys 475, and Cys 478 (Figure 1). However, given the higher affinity of zinc for the sulfur atom in Cys relative to the oxygen atom in Thr,

* To whom correspondence should be addressed: Fax (609) 258-6746; email glm@princeton.edu.

[‡] Department of Chemistry.

[§] Department of Molecular Biology.

[||] Present address: Office of the President, Rockefeller University, New York, NY 10021-6399.

10.1021/bi980596r CCC: $15.00
Published on Web 11/11/1998

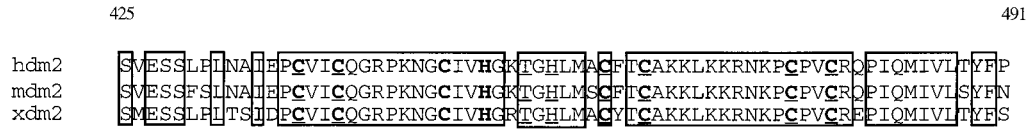

FIGURE 1: Amino acid sequence of hdm2 C-terminal domain containing the RING finger sequence and a comparison to its homologues in mouse (mdm2) and *Xenopus* (xdm2) (*41*). Conserved residues are boxed. The numbers labeled refer to the positions in the human sequence. The ligands involved in Zn^{2+} binding suggested by Boddy and Freemont (*6*) are underlined, and the ligands that we propose to be necessary are in bold face type.

and the fact that there is another Cys 449 and His 451 pair adjacent to the Thr 455 and His 457 pair, it seems chemically unlikely that Thr 455 substitutes for the third cysteine.

The C-terminal domain of the hdm2 protein was found to exhibit specific RNA binding ability (*19*). A SELEX[1] procedure yielded a subset of RNA molecules that bind efficiently to hdm2, among which a family of similar clones (clone A RNA) accounted for 78% of the molecules detected in this assay. Furthermore, it was demonstrated that the C-terminal 396−491 residues of hdm2 (containing the RING finger motif) was sufficient for the specific RNA recognition. This suggests the RING finger is a novel RNA-binding motif (*20*). The affinity for specific RNA ligands of hdm2 may further contribute to its role in regulation of cell growth and/or its oncogenic potential.

In the present work, we report detailed studies of the hdm2 C-terminal domain. The questions addressed include the following: (1) Does hdm2 bind zinc as a RING finger motif, and is the unusual Thr coordination involved? (2) What are the binding constants for metal? (3) What structural features does the C-terminal domain of hdm2 have in the absence and presence of zinc(II)? (4) What is the minimal RNA binding domain? (5) Is metal binding required for RNA binding?

MATERIALS AND METHODS

Peptide Synthesis and Quantitation. A peptide comprising of amino acids 425−491 of the hdm2 protein was synthesized and purified by the Synthesis and Sequencing Facility, Princeton University. The identity of the peptide was confirmed by mass spectrometry (MALDI). A variant peptide with Cys residues at positions 438 and 461 simultaneously changed to Ser (referred to as hdm2-Δsite1) and another peptide with a Cys to Ser mutation at 449 and a His to Gln mutation at 452 (referred to as hdm2-Δsite2) were synthesized and purified by the same facility. The concentrations of these peptide solutions were determined by their absorbance based on estimation from their amino acid composition (ϵ is estimated to be 1450 M^{-1} cm^{-1} at 276 nm) (*21*). The subsequent buffer used for the metal binding analysis was similar to the RNA binding buffer (20 mM Tris buffer, pH 7.5, and 150 mM NaCl in the absence of the Nonidet P-40, glycerol, and DTT), which was thoroughly degassed with Ar. All the peptide solutions and metal solutions were prepared in an anaerobic environment. $ZnCl_2$, $Co(NO_3)_2$, and $CdCl_2$ were dissolved in pH 2 H_2O/HCl solution.

Ellman's Test. To determine the concentration of reduced cysteines in the peptide, Ellman's test was conducted in 50 mM Tris-HCl buffer at pH 8.0 (*22*). An extinction coefficient of 14 150 M^{-1} cm^{-1} of TNB^{2-} at 412 nm was used to estimate the amount of reduced thiols that reacted with DTNB, resulting in the release of TNB^{2-} (*23*). A fully reduced hdm2(425−491) peptide would be expected to have seven reduced cysteines. Ellman's test showed that in the peptide solution prepared in the glovebox, only ∼5.5 equiv of reduced cysteines were present, corresponding to ∼78% of the cysteine ligands in a reduced form. The presence of the partially oxidized peptide could not be avoided by the simple addition of an excess of reducing agent like DTT, since DTT forms a brown complex with Co^{2+} that interferes with these studies. Ultimately, we chose to use the peptide for which reduced cysteine concentration could be reproducibly measured to avoid further complications from additional chemical manipulations. Thus, all the binding constants reported are based on the concentrations of reactive peptide calculated by Ellman's tests.

Cobalt Titration by UV Absorbance. Cobalt titration was performed on the hdm2(425−491) peptide monitored by optical spectroscopy over a range of 200−800 nm on a Perkin-Elmer Lambda 9 spectrometer. Increase of UV absorbance at three different wavelengths (690, 700, and 730 nm) were used for the spectral analysis. Peptide concentrations were 200−250 μM in Tris-HCl buffer, pH 7.5. During the titration, the cobalt concentration was raised from 0 to 5 times that of the peptide in a stepwise manner under positive Ar pressure.

Cobalt Titration by Tyrosine Fluorescence. The quenching of the fluorescence of the Tyr 489 in the hdm2(425−491) peptide upon binding to Co^{2+} was monitored on a QuantaMaster fluorometer (PTI, South Brunswick, NJ) arranged in an L format. The excitation wavelength was set to 272 nm, while the emission spectra were collected from 290 to 360 nm. The temperature (25 °C) was controlled by an external circulating water bath. The peptide concentrations used were 5 and 20 μM, which had absorbances below 0.05 at both the excitation and the emission wavelengths. For the quantitative analysis, a series of the peptide solutions were made at 5 μM under Ar with the Co^{2+} concentration increased from 0 to 20 equiv. Background-corrected fluorescence intensity at 300 nm was averaged in a 60 s time period and used for quantitative analysis. The relative change in fluorescence intensity as a function of the added Co^{2+} concentration was fitted to a 1:1 binding scheme to the following equation using Kaleidagraph:

[1] Abbreviations: SELEX, systematic evolution of ligands by exponential enrichment; PCR, polymerase chain reaction; SDS−PAGE, sodium dodecyl sulfate−polyacrylamide gel electrophoresis; CD, circular dichroism; NMR, nuclear magnetic resonance; GST, glutathione S-transferase; GdnHCl, guanidine hydrocholoride; DTT, dithiothreitol; DTNB, 5, 5′-dithiobis(2-nitrobenzoic acid); TNB, thionitrobenzoate; mAB, monoclonal antibody; IEEHV, immediate early equine herpes virus.

$$P\mathrm{Co}_{eq} = \frac{\Delta\text{fluorescence},i}{\Delta\text{fluorescence,total}} = \frac{(P_t + K_1 + [\mathrm{CO}^{2+}]_i) - \sqrt{(P_t + K_1 + [\mathrm{CO}^{2+}]_i)^2 - 4P_t[\mathrm{Co}^{2+}]_i}}{2P_t}$$

where $P_{|t}$ is the total concentration of active peptide that could bind Co^{2+}, K_1 is the dissociation constant, and $[Co^{2+}]_i$ is the concentration of added Co^{2+} at any point. Both K_1 and P_t were obtained by the fitting.

Circular Dichroism of hdm2(425−491). Circular dichroism of the hdm2(425−491) peptide was measured with an Aviv 60DS spectrometer. Spectra were recorded from 260 to 197 nm at 25 °C. Samples were prepared in the Tris-HCl buffer, and the peptide concentration was 50 μM. Samples with 1 and 2 equiv of $ZnCl_2$ were prepared separately.

Fluorescence Resonance Energy Transfer. In the Förster theory of energy transfer, the Förster distance R_0 where 50% energy transfer occurs is calculated from the spectral properties of the donor and acceptor chromophores as follows:

$$R_0 = 9.79 \times 10^3 (JQ_d\eta^{-4}\kappa^2)^{1/6} \quad (1)$$

where η is the refractive index of the medium and κ^2 is the orientation factor between the donor and the acceptor dipole moments. In the case of Co(II) being the acceptor, κ^2 was assumed to be $^2/_3$ (*24*, *25*). The quantum yield Q_d of the donor was determined to be 0.11 by comparison with *N*-acetyltyrosine amide (0.14) as a standard (*26*−*29*). The spectral overlap integral between the emission spectrum of the donor and the absorption spectrum of the acceptor was approximated by the following summation:

$$J\ (\mathrm{M}^{-1}\ \mathrm{cm}^3) = \frac{\int F_d(\lambda)\epsilon_a(\lambda)\lambda^4\ \mathrm{d}\lambda}{\int F_d(\lambda)\ \mathrm{d}\lambda} \quad (2)$$

where $F_d(\lambda)$ and $\epsilon_a(\lambda)$ are the relative fluorescence intensity (percent) of the donor and the molar extinction coefficient (molar^{-1} centimeter cm^{-1}) of the acceptor, respectively, and λ is the wavelength (centimeters).

The efficiency of energy transfer can be calculated from the steady-state intensities of the donor alone (I_d) and the donor−acceptor pair (I_{da}) molecules:

$$E = 1 - \frac{I_{da}}{I_d} \quad (3)$$

For a single donor and acceptor separated by a single distance, the experimentally measured values of E and R_0 are used to calculate the distance r:

$$E = \frac{R_0^6}{R_0^6 + r^6} \quad (4)$$

Expression of GST-Fused hdm2 C-Terminal Fragments. The deletion fragments were constructed by PCR amplification of the RING finger domain from pBlueRel [(hdm2(1−491)], which has hdm2 inserted into the *Eco*RI site of pBluescript KS$^-$ (*13*). The following oligonucleotides were used to generate the desired fragments:

415(+)	CGGAATTCGAAAGGGAAGAAACC
425(+)	CGGAATTCAGTGTGGAATCTAGT
434(+)	CGGAATTCGCCATTGAACCTTGT
480(−)	GTCTCGAGGCTATGCTCTACATACTGG
491(−)	GTCTCGAGGCTAGGGGAAATAAGT

The fragments containing hdm2(415−491), (425−491), (434−491), (415−480), (425−480), and (434−480) were digested with *Eco*RI and *Xho*I, and inserted into the *Eco*RI- and *Xho*I-digested pGEX-4T-1 vector (from Pharmacia). The fragments with a truncated C-terminus at 480 have a Gln to Ala mutation at position 480. The presence of these fragments were confirmed by sequencing their ds DNA using automated fluorescence methods performed by the Synthesis and Sequencing Facility in Princeton University. The mutant proteins were expressed in BL21 cells in LB medium. It is worth noting that if the last 11 mostly hydrophobic amino acids on the C-terminus (481−491) are present, a growth temperature of 30 °C has to be used for soluble protein expression. When these 11 amino acids are deleted, soluble proteins can be obtained at a growth temperature of either 30 or and 37 °C. The cells were harvested after induction with 0.1 mM IPTG for 2 h. Purification of the GST-fused hdm2 RING finger proteins was performed by lysing the induced cells by sonication, and isolating with glutathione−agarose beads (Pharmacia). Approximately 6−40 mg/L purified proteins can be obtained from this method. The purity of each fragment appears to be >95% as judged from SDS−PAGE analysis. Western blot analysis was carried out with GST−hdm2(415−491) and GST−hdm2(425−491) with 2A10, 4B11, and 5B10 monoclonal antibodies and with polyclonal antibody. Quantitation of the GST−fusion proteins was done with the Bradford assay (reagents from Biorad). A soluble GST−fusion protein, GST−CSB [a GST−fusion protein containing amino acids 1−242 of CSB DNA repair ATPase (*14*)], was used as a control both for protein expression and (negative) RNA binding.

Mutagenesis of the GST−hdm2(396−491) Fragment. The single mutation containing GST-fused hdm2(396−491) was obtained by the unique site elimination method (*30*) (kit from Pharmacia) and the PCR overlap-extension method (*31*). The following oligonucleotides were used to direct the mutations by the unique site elimination method:

C438S(−)	pdAATCACAGAAGGTTCAATGG
C475S(−)	pdACATACTGGGGAGGGCTTATTCCT

The PCR overlap-extension method was used to incorporated these mutations in the GST hdm2(396−491) DNA. The following oligonucleotides were used:

H457Q(+)	AAAACAGGACAGCTTATGGCC
H457Q(−)	GGCCATAAGCTGTCCTGTTTT
C461S(+)	CTTATGGCCTCCTTTACATGT
C461S(−)	ACATGTAAAGGAGGCCATAAG

The presence of the mutations was confirmed by sequencing. The mutant protein were expressed and purified as described.

RNA Binding Assays. RNA binding assays were carried out following the procedure developed by Elenbaas et al. (*19*). Briefly, a 77-nt template oligonucleotide was amplified by PCR and then used to transcribe the clone A RNA derived from a SELEX procedure. The DNA template was purified by phenol extraction and ethanol precipitation. The transcription was carried out with 200 ng of DNA template using T7 RNA polymerase from U.S. Biochemical Corp. [α-^{32}P] UTP (25 μCi) (Amersham) was used to label the RNA for a 50 μL reaction. Free nucleotides were removed by passing the reaction mixture through a G-50 spin column (Pharmacia).

The binding reactions were carried out by incubating 50 μg of GST-fused hdm2 fragments on GST agarose beads in a total volume of 300 μL of RNA binding buffer (20 mM Tris-HCl, pH 7.5, 150 mM NaCl, 0.1% Nonidet P-40, 2% glycerol, and 1 mM DTT) with ~0.1 μg of ^{32}P-labeled RNA and 20 μg each of unlabeled poly(U) RNA and yeast RNA (Sigma) as nonspecific competitors. RNA binding reactions were carried out at room temperature for 1 h with rotating, followed by three washes in RNA binding buffer, after which the beads were resuspended in 80 μL of buffer and radioactive RNA bound to the GST-fused hdm2 was counted by scintillation.

Fifty micrograms of the chemically synthesized hdm2-(425−491) peptide was immunoprecipitated with 50 μL of 50% protein A−Sepharose beads, 250 μL of mAB supernatant and 200 μL of lysis buffer (50 mM Tris-HCl, pH 7.5, 150 mM NaCl, 0.5% Nonidet P-40, and 1 mM DTT) at 4 °C overnight. The RNA-binding procedures were carried out as described. To investigate the role of metal in RNA binding, all the buffers were treated with Chelex-100 (Sigma) before any divalent ions (Mg^{2+} or Zn^{2+}) were added.

RESULTS

Previous studies have shown that hdm2 binds specifically to RNA selected from a SELEX procedure (*19*). A C-terminal fragment of hdm2(396−491) was employed to prove that the RING finger domain of hdm2 is sufficient for specific RNA binding. Studies on truncated fragments revealed that amino acids 425−491 are essential for RNA recognition (see later). Therefore, a synthetic hdm2 peptide containing residues 425−491 was employed in our study.

Metal Binding to the hdm2(425−491) Peptide. Divalent metal binding properties of the hdm2(425−491) peptide were determined by studying the optical absorption spectra of the cadmium−peptide and the cobalt−peptide complexes. The spectra of the cadmium−peptide complex are shown in Figure 2. A characteristic Cd(II)−S charge transfer band was observed approximately at 250 nm. The presence of this band not only suggests that Cd^{2+} binds to the peptide but also indicates that at least one of the coordinating residues is a cysteine (*32, 33*).

Cobalt(II) has been used extensively as a spectroscopic probe in zinc-containing proteins to study the coordination geometry and ligand type (*34, 35*). It forms complexes isostructural to the corresponding zinc(II) complexes with binding affinities ca. 3 orders of magnitude lower than those of the zinc complexes. The UV−visible spectra of hdm2-(425−491) is shown in Figure 3A. The spectrum contains a d−d absorption envelope in the visible region with maxima

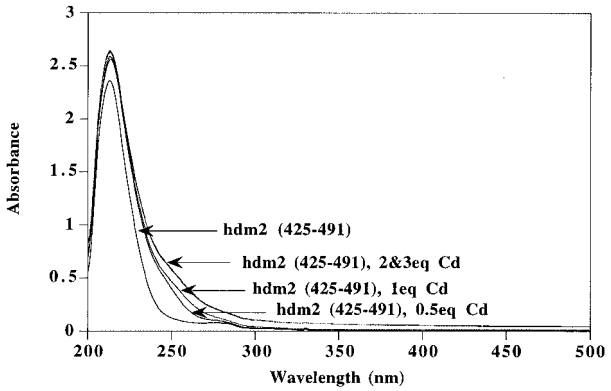

FIGURE 2: Cadmium(II) binding to hdm2(425−491) as monitored by UV absorbance.

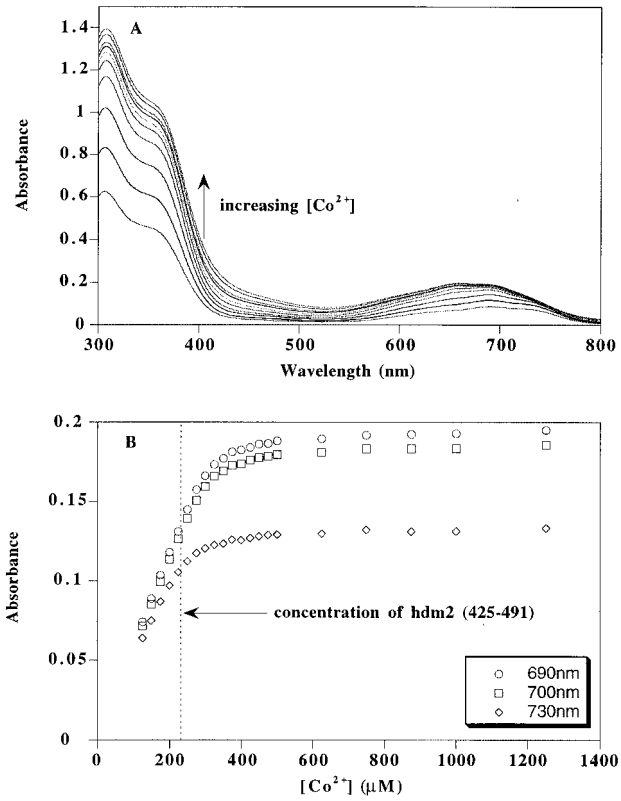

FIGURE 3: Titration of Co(II) to hdm2(425−491) as monitored by UV absorbance. (A) UV spectra from 300 to 800 nm at different Co(II) concentrations. (B) Changes in UV absorbance monitored at single wavelengths.

at approximately 650, 695, and 730 nm. This spectrum is consistent with those of other Co^{2+}-substituted proteins with a tetrahedral coordination site. In addition, thiolate−Co^{2+} charge-transfer bands are observable at about 310 and 360 nm, indicating the presence of at least one cysteine residue as a donor (*34*). Also, Co(II) was readily displaced by Zn-(II) as evidenced by the disappearance of the absorbance band in the range of 500−800 nm, indicating the preferential binding of the peptide to zinc over cobalt (not shown).

A direct titration of Co^{2+} to the hdm2(425−491) peptide was performed. A typical trace followed by UV absorbance is shown in Figure 3B. These spectra are corrected for dilution effects. The absorbance increased linearly at the beginning of the titration; after 1 equiv of Co^{2+} was added, the increase in absorbance started to deviate from linearity; after about 3 equiv of Co^{2+}, the change in absorbance became

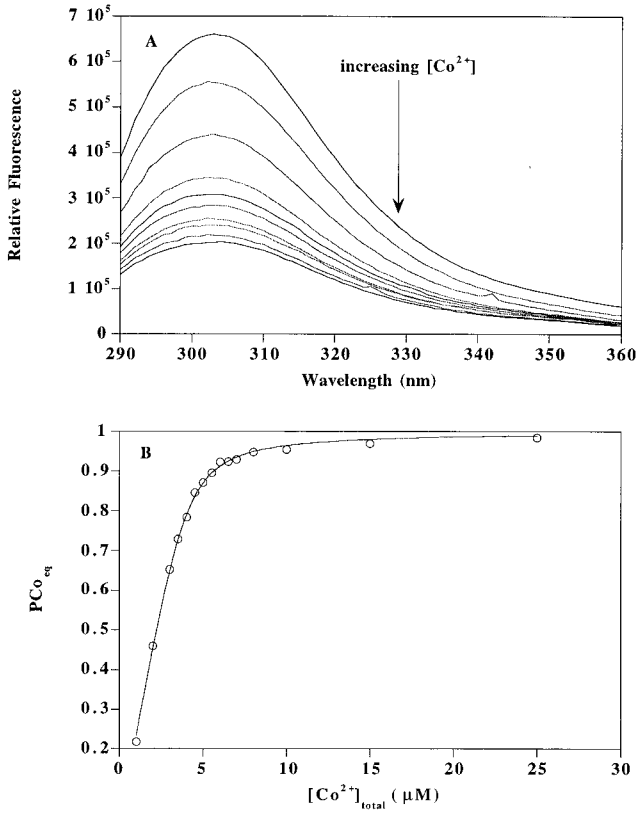

FIGURE 4: (A) Titration of Co(II) to hdm2(425−491) monitored by emission spectra of tyrosine fluorescence, $\lambda_{ex} = 272$ nm. (B) Changes in fluorescence intensity at 300 nm were used to calculate the fraction of Co(II) bound to site 1. The solid line represents fitting using a 1:1 binding model.

rather small and could be treated as a posttransitional region. The extrapolation of the linear portion at the beginning of the titration and the posttransitional baseline gave the approximate stoichiometry of Co^{2+} binding. This number consistently turned out to be about 1.4 equiv of Co^{2+}/ total peptide. This raised some uncertainties as to whether hdm2-(425−491) bound to 1 or 2 equiv of Co^{2+}. However, since oxidized thiols cannot bind metal, and some oxidation is usually present in cysteine-rich peptides, a correct stoichiometry requires assessment of reduced thiol concentration.

Ellman's test was carried out on the hdm2(425−491) peptide and only 78% of the cysteine ligands are shown to exist in a reduced form. If we assume that the 22% oxidized cysteine ligands would result in a 22% reduction in the amount of Co^{2+} bound, the stoichiometry we determined at 1.4 equiv of Co^{2+}/peptide should be about 1.8 equiv of Co^{2+}/ peptide, i.e., the hdm2 peptide is likely to bind two Co^{2+}. A second line of evidence came from coupling absorbance measurements with the tyrosine fluorescence study described below. Together these experiments clearly demonstrate the presence of two metal binding sites in the hdm2 C-terminal domain.

Cobalt Binding to hdm2(425−491) Monitored by Tyrosine Fluorescence. The hdm2(425−491) peptide contains only a single Tyr at position 489 close to its carboxyl terminus. When the peptide was excited at 272 nm, an emission spectrum characteristic of tyrosine with a maximum around 300 nm was observed (Figure 4A). At a peptide concentration of 20 μM, when Co^{2+} was titrated into the solution, the tyrosine fluorescence decreased steadily until a plateau was reached at 0.9 equiv after correcting for oxidized peptide, and no further quenching could be observed. Although this may seem inconsistent with the 1.8 equiv of Co^{2+}/peptide we obtained from the UV-monitored binding, in fact only one of the two bound zinc is expected to be observed by this method. The Co^{2+}−peptide complex absorbs around 300 nm as a result of Co^{2+}−sulfur charge transfer (*36*). This absorbance overlaps with the tyrosine fluorescence emission (*37*), and therefore, energy transfer occurs between the tyrosine and the metal center. Since energy transfer efficiency has a r^6 dependence (where r is the donor−acceptor distance), most likely only the metal center that is close to the tyrosine in space can be observed. This observation strongly supports a model of two metal binding sites with different affinities in the hdm2 C-terminal domain. Fluorescence binding methods monitor the strong binding site. (If the weaker binding site were close to Tyr 489 in space, changes in fluorescence would only occur after 1 equiv of Co^{2+} was titrated.) From the characteristic absorbance of this site, we assign this site as a C_4 site by comparison with the BRCA1 RING finger domain (*4*).

Quantitative Analysis of Cobalt Binding to hdm2(425−491) Peptide. Quantitative analysis of fluorescence monitored binding was carried out on a series of hdm2(425−491) solutions at 5 μM with the concentration of Co^{2+} ranging from 0 to 20 equiv (Figure 4B). A conventional titration method was not used because the fluorescence intensity of the peptide and the Co^{2+}−peptide complex can decrease upon repeated exposure to the excitation light beam. From the fitting, K_1 was found to be $(2.2 \pm 0.2) \times 10^{-7}$ M. This value is remarkably similar to that of the BRCA1 RING finger peptide ($\log K_1 = -7.6 \pm 0.7$) (*4*). The total active peptide concentration found by fitting was 3.9 ± 0.1 μM, corresponding to ∼78% peptide capable of binding to Co^{2+}. (This agrees with our Ellman's test, which showed that around 78% of the thiols were reduced.) The total decrease of fluorescence was 73%. This can be utilized to estimate the donor−acceptor distance between Tyr 489 and the Co^{2+} at site 1.

With the dissociation constant K_1 in hand, we could examine the UV-monitored Co^{2+} binding data more closely. The absorption spectra in the range of 500−800 nm at different Co^{2+} concentrations were plotted in Figure 5A. The concentration of hdm2 (425−491) was 230 μM in this example. At Co^{2+} concentrations below 200 μM, the absorption spectra exhibited a maximum around 690 nm, with two shoulders around 630 and 730 nm. This matches the absorption spectrum assigned for site 1 in Roehm and Berg's study of the BRCA1 RING finger peptide (site 1 is the C_4 site with a higher affinity for Co^{2+}) (*4*). At Co^{2+} concentrations higher than 300 μM, the absorption spectral shape changed. The increase in intensity around 650 nm was larger than at 690 and 730 nm. At 1 mM Co^{2+}, 650 nm became the wavelength where the maximum resided, with two shoulders at 690 and 730 nm. This clearly suggested that a second transition took place that had different characteristics in absorption.[2] Due to the large differences in binding affinity of different subsites, the basis spectra of each could readily be obtained. Assuming that metal binding to site 1 and 2 is independent and that $K_1 \ll K_2$, site 1 would be preferentially filled at a peptide concentration of 230 μM (1000 times higher than K_1).

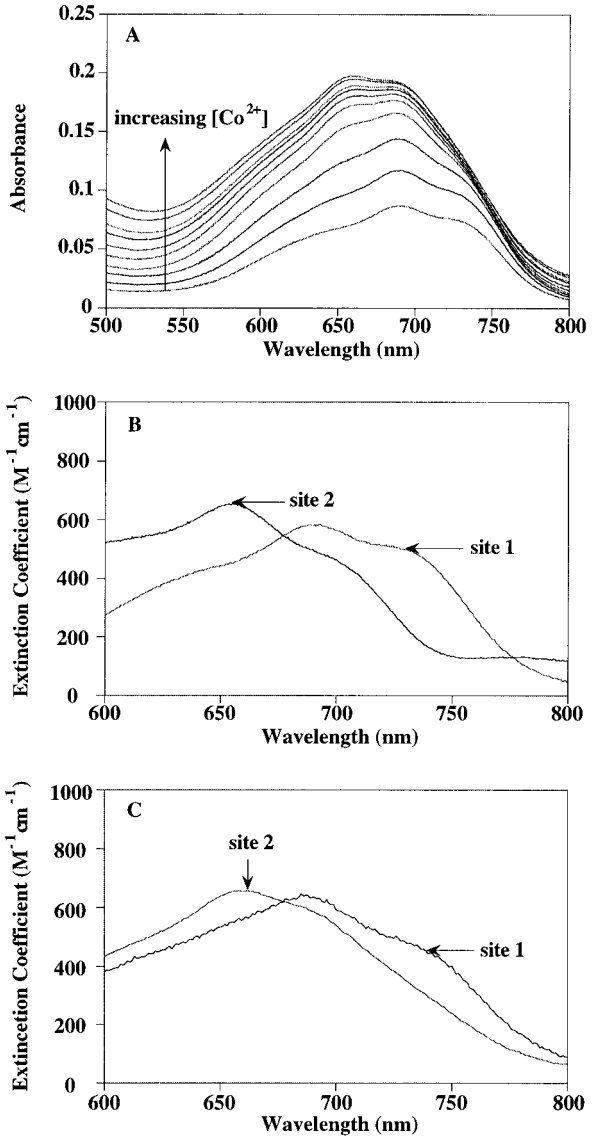

FIGURE 5: Resolution of the absorbance spectra of Co(II)-hdm2 to two basis spectra. (A) UV absorption spectra at 500−800 nm with various concentrations of cobalt(II). (B) Estimated spectral contribution of Co(II) bound to hdm2 at site 1 and site 2 obtained with our assumptions that K_1 and K_2 are independent and $K_1 \ll K_2$. (C) Spectral contribution of Co(II) bound to hdm2 at site 1 and site 2 from hdm2-Δsite2 and hdm2-Δsite1 mutant peptides (peptide/Co^{2+} = 1), respectively.

Therefore, the initial absorbance results from the binding of Co^{2+} to site 1 exclusively. We also assume that at 1 mM Co^{2+} most of the second site is occupied and that the absorption spectra could be treated as the sum of the absorption due to Co^{2+} in sites 1 and 2. We obtain a residual absorption spectrum for site 2 after the contribution of site 1 is subtracted from the total. The extinction coefficients obtained this way were plotted in Figure 5B. For these estimates, the magnitude of the extinction coefficient may not be accurate, but the spectral position and shape should accurately represent the characteristics of the absorption resulting from Co^{2+} binding to hdm2 at sites 1 and 2,

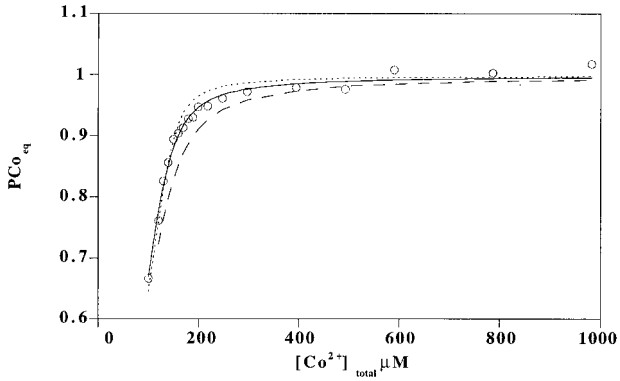

FIGURE 6: K_2 is obtained from Co(II) titration of the hdm2-Δsite 1 peptide followed by UV absorbance; the solid line represents fitting to a 1:1 binding model, which gives a K_2 of 3.7 μM. When a K_2 of 2 μM (dotted line) or 6 μM (dashed line) is used, a satisfactory fit cannot be obtained.

respectively. The contribution from both sites 1 and 2 using these approximations are very similar to Roehm and Berg's results from both factor analysis and mutant peptide studies (*4*).

With our assumptions that K_1 and K_2 were independent, that $K_1 \ll K_2$, and also that only 78% of the peptide was reduced, we subtracted the contribution from the binding to site 1 from our estimates shown in Figure 5B and fitted this with a 1:1 binding scheme. An estimate of 10−20 μM for K_2 was obtained, which was 50−100 times higher than K_1, demonstrating that the key approximation ($K_1 \ll K_2$) is reasonable. This value falls in the range of the dissociation constant for site 2 of the BRCA1 peptide (8 ± 2 μM) when site 1 is occupied (*4*).

As already noted, use of Thr 455 as a ligand seems chemically unlikely. We alternatively hypothesized that Cys 449 and His 452 would bind the metal. The nature of the two binding sites was tested by two synthetic mutant peptides. In the first, two of the ligands in the high-affinity site (site 1), were changed to serine, C438S and C461S. In the second, C449S and H452Q mutations were made. These mutated peptides are referred to hereafter as hdm2-Δsite1 and hdm2-Δsite2, respectively. Titration of both peptides with Co(II) was carried out by UV absorbance as described. Both peptides bound to approximately 1 equiv of metal ion after correcting for reduced thiols. Figure 5C represented the absorption spectra of the mutant peptides in the presence of 1 equiv of Co(II). In the case of hdm2-Δsite1, at 1 equiv of Co(II), the spectral line shape and position are similar to the assigned low-affinity C_3H site.[3] The increase in intensity of this absorbance spectrum was fitted to a single binding scheme, which yielded a dissociation constant of 4 ± 1 μM (Figure 6). Assuming that this reflected the intrinsic affinity of site 2 when site 1 was unoccupied (K_d = 15 ± 5 μM when site 1 was occupied), metal binding to the hdm2 RING finger peptide is anticooperative as also found by Rochm and Berg (*4*) for BRCA1.

Similar binding studies on hdm2-Δsite2 yielded a characteristic absorption spectra in the presence of 1 equiv of

[2] The factor analysis method used by Roehm and Berg (*4*) failed to resolve the change in absorption to two expected basis spectra. This failure could arise from many sources, including the presence of the partially oxidized peptide or the oxidation of a small portion of the peptide during the course of the titration.

[3] When Co(II) concentration was less than 0.5 equiv of the reduced peptide, an apparent 2:1 peptide−Co(II) species was present as observed in the C_2H_2 minimalist peptide previously (*28*). This evolved to a C_3H spectrum at higher Co(II) concentration. Above 1 equiv, additional Co^{2+} did not change the spectral shape and position.

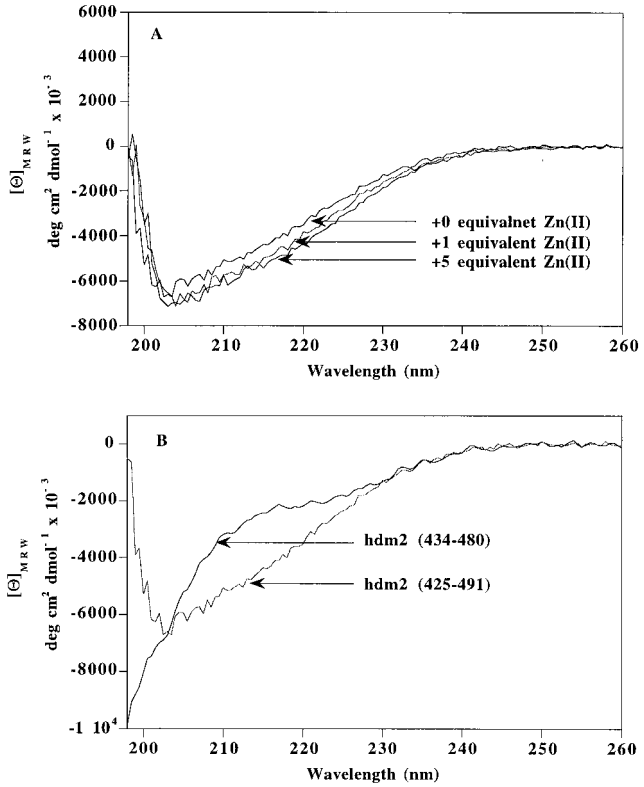

FIGURE 7: Far-UV CD spectra of (A) hdm2(425−491) peptide in the presence and absence of Zn(II) and (B) hdm2(425−491) and hdm2(434−480) peptide in comparison in the absence of Zn(II).

cobalt(II) (Figure 5C). The absorbance spectrum of the complex of hdm2-Δsite2 with Co^{2+} only changed amplitude but did not change shape from 0 to 1 equiv of cobalt(II). At higher Co^{2+} concentrations, the absorbance at key wavelengths (for example, 690 and 730 nm) remains constant, which vary for the wild type when site 2 is occupied. If the proposal of Freemont et al. were correct, mutations in Cys 449 and His 452 should not affect Co^{2+} binding at all; i.e., this peptide should exhibit the same binding profile as the wild-type peptide. However, this mutant peptide only binds 1 equiv of Co^{2+} instead of 2, and the resulting spectrum was that expected for the high-affinity C_4 site.[4] The dissociation constant for Co(II) binding to the C_4 site was found to be in the submicromolar range, consistent with the result from fluorescence energy transfer, which gave a K_1 of 0.22 μM.

Through these studies, we have demonstrated that the C-terminal domain of hdm2 indeed contains a RING finger domain that binds to metal sequentially and anticooperatively. The two metal binding sites consist of a C_4 site and a C_3H site; the proposed Thr for Cys substitution in the C_3H site was incorrect. Next, we carried out structural characterizations on the hdm2(425−491) fragment to investigate the role of zinc in folding of the hdm2 RING finger domain.

Circular Dichroism of the hdm2(425−491) Peptide. The CD spectra of hdm2(425−491) peptide in the presence and absence of Zn^{2+} are shown in Figure 7A. The spectra suggest that there is minimal secondary structure present in the hdm2(425−491) peptide. The presence of 1 and 2 equiv of Zn^{2+} induced a small but noticeable change, suggesting the presence of some metal-induced structure (Figure 7A). The CD spectrum of the hdm2(434−480) peptide, which does not bind to RNA, is shown in Figure 7B in comparison with the hdm2(425−491) peptide. The hdm2(434−480) peptide exhibited a typical random coil-like spectrum with a minimum around 200 nm. The hdm2(425−491) peptide, in contrast, had more negative ellipticity around 220 nm and less around 200 nm, suggesting the presence of some sort of structure, most likely β-turns.

Fluorescence Resonance Energy Transfer Studies. The distance between the energy donor (Tyr 489) and the energy acceptor (Co^{2+} bound to hdm2 at site 1) was determined by the fluorescence resonance energy transfer technique. The sufficient spectral overlap at about 300 nm ensures efficient energy transfer from the donor to the acceptor (*36*, *37*). The value of R_0 for energy transfer from Tyr 489 to Co^{2+} at site 1 was calculated to be 21 Å. The uncertainty in the determination of the extinction coefficient of Co^{2+}−hdm2 complexes affects the R_0 only slightly from eqs 1 and 2. Even when the extinction coefficient of Co^{2+}−hdm2 with both sites 1 and 2 occupied was used, R_0 was calculated to be 23 Å. As we discussed before, 73% of the fluorescence was quenched while only 78% of the peptide was able to bind to Co^{2+}. As expected, the fluorescence intensity of the oxidized peptide was unchanged in the presence of Co(II). The residual 27% fluorescence intensity observed upon Co(II) addition should thus be largely assigned to the 22% partially oxidized peptide. By this analysis, the energy transfer efficiency was estimated to be 90% (±10%). A distance of 14 ± 2 Å is obtained, assuming 80−95% quenching. This result demonstrates that Tyr 489 is close in space to binding site 1 even though site 2 is closer in primary sequence, suggesting that the peptide exists in a compact conformation, at least in the presence of the metal ions.

To further probe this compact structural feature, fluorescence energy transfer was measured in 3.8 M GdnHCl. The UV absorption spectra indicated that Co^{2+} remained bound to the peptide at GdnHCl concentrations as high as 5 M. However, the quenching effect of Co^{2+} binding diminished in the presence of 3.8 M GdnHCl. In the presence of 20 equiv of Co^{2+}, the fluorescence intensity only decreased by ∼5%, suggesting a much longer Co^{2+}−Tyr 489 distance (>30 Å) (data not shown). Therefore, it appears that the foldback of the hydrophobic tail (481−491) of the hdm2-(425−491) peptide can be disrupted by the presence of denaturant.

The structural studies suggest that hdm2 exists in a compact conformation without a lot of regular secondary structures, and the addition of zinc did not seem to nucleate a major folding event. Next, we investigated the RNA binding properties of the hdm2 RING finger domain and the effects of metal binding on the RNA recognition.

Expression and RNA Binding of hdm2 C-Terminal Deletion Mutants. To screen for the shortest hdm2 fragment required for RNA recognition, fusion proteins of glutathione S-transferase (GST) and the deletion sequences of the hdm2 RING finger domain (415−491), (425−491), (434−491), (415−480), (425−480), and (434−480) were constructed and expressed in *Escherichia coli.*

[4] At high Co^{2+} concentrations, a small increase in absorbance at 650 nm is observed; this could be a result from Co^{2+} binding to the remaining His 457, Cys 461, and Cys 464 in a tetrahedral coordination site with water or the −OH group from Thr 455 as the fourth ligand.

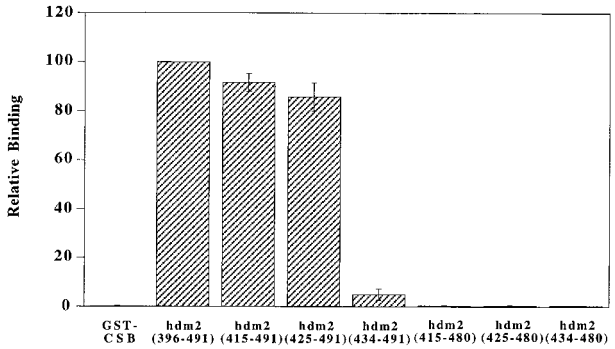

FIGURE 8: ^{32}P-labeled RNA (clone A from the SELEX procedure) binding to GST-fused hdm2 fragments in 20 mM Tris-HCl, pH 7.5, with 150 mM NaCl, 1 mM DTT, 0.1% NP-40, and 2% glycerol. The amount of radioactivity was normalized to the level bound to hdm2(396−491).

RNA binding utilizing the predominant RNA molecule, clone A, from the SELEX procedure was carried out on the hdm2 C-terminal deletion mutants following the procedures developed by Elenbaas et al. (*19*) (Figure 8). Approximately 20−30% of the radioactivity was retained after 3 washes with the RNA binding buffer. The binding of the original fragment (396−491) was included as a standard for comparison. The binding of fragments (415−491) and (425−491) were very similar to the original fragment (396−491). Fragment (434−491) only bound 5%, indicating that the 10 amino acids (425−433) are critical for binding and/or folding. Interestingly, when the last 11 hydrophobic amino acids were truncated, the yield of the purified proteins increased severalfold, while the RNA binding of these fragments was abolished. This would suggest that these last 11 amino acids play an active role in mediating the folded structure of this peptide or directly participate in interaction with the RNA.

Metal Requirement for RNA Binding to hdm2. In the original assay, 5 mM $MgCl_2$ and 50 μM $ZnCl_2$ were added to the RNA binding buffer (*19*). In the course of this study, it became clear that the addition of these divalent ions was not absolutely necessary for RNA binding. In fact, the addition of zinc(II) made the experiments less reproducible, presumably due to the catalytic activity of zinc(II) in mediating RNA hydrolysis. Experiments were carried out using the GST-fused hdm2(396−491) protein in the absence and presence of additional Mg^{2+}, Zn^{2+}, and EDTA. Indeed, RNA binding by hdm2 occurs even in the absence of any additional Mg^{2+} and Zn^{2+} and in the presence of EDTA as high as 10 mM (not shown).

To investigate the possibilities that Zn^{2+} might be supplied by *E. coli* during growth and that there might be a kinetic barrier for the additional EDTA to remove the bound Zn^{2+} from the GST-fused proteins, synthetic peptide fragment hdm2(425−491) was employed in the study. This fragment was immunoprecipitated with a monoclonal antibody 4B11 that is specific for the C-terminal domain of hdm2, and the RNA binding assay was carried out as described. The peptide solution was prepared in the glovebox where DTT was added to make the final concentration 1 mM, after which the solution was manipulated under air. All the solutions were treated with Chelex-100 resin to remove any divalent metal ions. The immunoprecipitated peptide was found to bind to RNA regardless of the presence of Zn^{2+} or 5 mM EDTA. This strongly suggests that Zn^{2+} is not required for RNA binding.

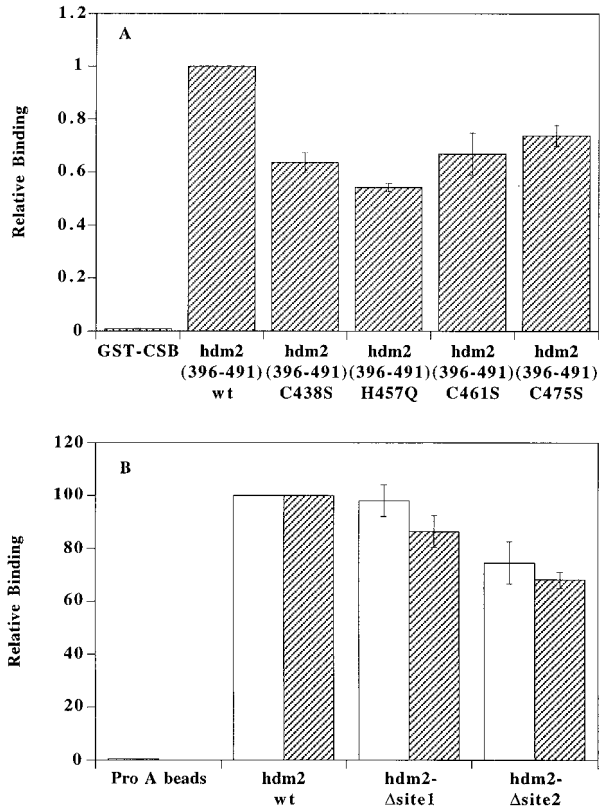

FIGURE 9: Metal requirement of RNA binding to hdm2. (A) Relative binding of GST-fused hdm2(396−491) point mutants to clone A RNA in RNA binding buffer without additional Zn(II) or Mg(II). (B) Relative binding of clone A RNA and a fragment of human ribosomal RNA (shaded columns) to immunoprecipitated wild-type hdm2(425−491) and hdm2-Δsite1 and hdm2-Δsite2 variant peptides.

Mutant hdm2 peptides with single amino acid substitutions (cysteine to serine or histidine to glutamine) were prepared on GST-fused hdm2(396−491) by site-directed mutagenesis. RNA binding assay was performed on these mutants. If a Zn^{2+}-mediated RING finger fold is the structure needed for RNA recognition, it is expected that if one of the two binding sites is eliminated by mutating one of the Cys or His ligands, the RNA binding affinity should be greatly reduced. As we demonstrated, Cys 438, Cys 441, Cys 461, and Cys 464 form binding site 1, while site 2 is created by Cys 449, His 452, Cys 475, and Cys 478. Therefore, the C438S and C461S mutants should abolish Zn^{2+} binding to the first binding site, while the C475S mutants should eliminate Zn^{2+} binding to site 2. An additional mutant containing the H457Q variation was also included in the study to test whether this His is critical in RNA binding. The result from the RNA binding assay demonstrated that all four of these mutants still bind to pHCS A RNA with 60−80% affinity comparing with the wild-type (396−491) fragment (Figure 9A).

The affinity of the two synthetic mutant peptide (hdm2-Δsite1 and hdm2-Δsite2) for the clone A RNA was also tested. The wild-type and the mutant peptides were immunoprecipitated with the monoclonal antibody 4B11. RNA binding assays were carried out as described. Metal binding sites 1 and 2 in the hdm2(425−491) peptide were destroyed, respectively, in the two peptides as demonstrated with the

cobalt(II) binding assay. The result from the RNA binding assay using the immunoprecipitated peptides is shown in Figure 9B. The mutant peptides, hdm2-Δsite1 and hdm2-Δsite2, still bind to the clone A RNA with similar affinity as the wild-type peptide. These results taken together strongly suggest that Zn^{2+} is not required for RNA binding.

In all the above experiments, the clone A RNA from the SELEX procedure (*19*) was employed for the binding assay. It was shown that a fragment of human ribosomal RNA (328−406) selected from a poly (A)-enriched library also binds to hdm2 (*18*). Experiments were carried out using this fragment of ribosomal RNA to test its affinity for the wild-type and the mutant peptides. In vitro transcription was used to obtain the ^{32}P-labeled ribosomal RNA from the DNA template of 154 bp containing a T7 promoter sequence. Binding assays were carried out accordingly. As shown in Figure 9B, this fragment of ribosomal RNA binds the wild-type, the hdm2-Δsite1, and the hdm2-Δsite2 peptide with similar affinity. From the percent of radioactivity retained in the binding assay, the ribosomal RNA seems to bind hdm2 with higher affinity than the clone A RNA from the SELEX procedure.

DISCUSSION

In a previous study, Elenbaas et al. (*19*) examined the RNA-binding activity of hdm2. Specific RNA ligands that bound to the hdm2 protein with high affinity were identified through a RNA SELEX procedure. This specific RNA binding was mapped to the C-terminal domain of hdm2 containing the proposed RING finger motif.

The cysteine-rich region between residues 438 and 478 at the C-terminus of hdm2 was initially proposed to have two tandem zinc fingers of the C_2H_2 and C_4 class, respectively (*10, 13*). Sequence alignment indicated that this region had significant homology to the RING finger motif, in which the two binding sites of the C_3H and the C_4 type fold into a single unit. A substitution of the third cysteine for Thr was also proposed, with the hydroxyl of the threonine replacing the sulfhydryl group of cysteine in the coordination of Zn^{2+} (*6*). As Vallee and Auld pointed out, once proteins that contain putative metal-binding domains are recognized, the presence, mode of binding, and role of metal ions must still be verified (*38*). We investigated the metal binding of the C-terminal domain of hdm2. By using absorption and fluorescence spectroscopy and taking advantage of comparison with the well-characterized BRCA1 RING finger domain (*4*), the C-terminal domain of hdm2 was found to bind two molecules of zinc(II) in an interleaved fashion analogous to the BRCA1 RING finger domain. However, the tertiary folded motif found in two other RING fingers is not present in hdm2. Furthermore, the previously suggested sequence alignment does not correctly identify the residues involved in metal ligation. The metal binding properties of two mutant peptides verified our approximation of the spectral contributions from cobalt(II) binding to hdm2 at sites 1 and 2. The C_3H site was demonstrated to consist of Cys 449, His 452, Cys 475, and Cys 478, rather than the proposed Thr 455, His 457, Cys 475, and Cys 478. Thus, the proposed Thr for Cys substitution in the C_3H site is not present. Instead, an adjacent ligand pair of Cys 449 and His 452 is likely used (Figure 1). This is reasonable considering the higher affinity of zinc(II) for sulfur rather than for oxygen. However, the periodicity the authors found of the conserved hydrophobic residues between the first and the third pair of ligands would be invalid (*6*). The second pair of ligands in hdm2 is Cys-X_2-His instead of the more common Cys-X-His (*2, 3*), which undoubtedly relieves some of the constraints caused by the short distance from the cysteine to the histidine residue (*39, 40*). These variations may account for a different packing pattern for the RING finger in hdm2 than previously found for structurally characterized RING peptides.

Although the preliminary metal binding properties of some RING finger domains were reported, BRCA1 represents the first example of RING finger proteins whose unique modes of metal binding were characterized in detail (*4*). Metal binding was demonstrated to be sequential, with site 1 nearly fully occupied before metal binding to site 2. A variant peptide revealed that metal binding is anticooperative; the metal binding to site 1 decreases the affinity of site 2. Analysis of the absorption spectra revealed that the higher affinity site is the C_4 site, while the lower affinity site is the C_3H site. In our study of hdm2, we were fortunate to be able to follow the metal binding to the stronger binding site by fluorescence energy transfer, which enabled us to evaluate the two binding events separately. By comparing the characteristic spectra of cobalt(II) bound in a tetrahedral site with ligand variations (*34*) and the BRCA1 peptide (*4*), we also assigned the stronger binding site to be the C_4 site and the weaker one to be the C_3H site. Synthetic knockout mutants not only enabled us to assign the coordinating residues in the hdm2 RING finger domain but also revealed that metal binding to hdm2 was also anticooperative. Thus, this sequential and anticooperative metal binding seems to be a general feature of the RING finger domains. This may prove to be important in the biological role of RING finger-containing proteins, since the RING finger domains may have one or both of the metal sites filled depending on which cellular compartment they are in and thus may perform different functions.

Two structures of RING finger motifs solved by ^{1}H NMR methods have been reported. Both have the characteristic cross-braced zinc ligation pattern and similar overall folding topologies. The IEEHV RING finger domain adopts a β-β-α-β fold (*40*), while the PML RING finger has a β-β-β-loop-$\alpha 3_{10}$-β fold (*39*). A number of conserved hydrophobic residues form the core of both structures. In both cases, Zn^{2+} binding appears to nucleate folding and stabilizes the tertiary structure. Preliminary studies on hdm2 by NMR spectroscopy suggested a lack of regular structural elements as judged by the absence of dispersion of the one-dimensional spectrum and the small number of cross-peaks in the 2D NOESY spectrum. The presence of zinc(II) did not seem to induce a major folding event. Though lacking in regular secondary structures, the structure of hdm2 in the presence of zinc(II) was not completely random as judged by the far-UV CD spectrum and by fluorescence energy transfer studies. Comparing with the BRCA1 peptide (*4*), the CD spectrum of the hdm2(425−491) fragment does not contain a significant amount of α-helix and does not change significantly upon Zn(II) binding. Fluorescence energy transfer was observed from the Tyr 489 near the C-terminus to the cobalt(II) bound in the higher affinity site (site 1). A distance of 14 ± 2 Å between the cobalt and Tyr 489 was estimated,

indicating that the peptide existed in a compact conformation, at least in the presence of the metal ions. We note that some other protein domains involved in cellular control functions, for example p21, do not adopt stable secondary and tertiary structures until bound to their cellular target receptors (J. Dyson, personal communication). Such "induced fit" may provide an additional level of functional control.

The RNA binding of hdm2 was further investigated in its relationship to the RING finger motif. The minimal length of the RNA binding domain was found to comprise residues 425−491. Although a stretch of basic residues (KKLKKRNK, 100% conserved from human to *Xenopus*, Figure 1) located between the third and fourth pairs of metal binding ligands in hdm2 were likely involved in the direct interaction with RNA, the RNA recognition seemed to require more than the presence of these basic residues. While the hdm2(434−480) peptide bound metal with similar affinity as the hdm2(425−491) peptide as judged by the absorption method, it did not have any affinity for the clone A RNA. One important difference is that this peptide adopts a totally random conformation as evidenced by its CD spectrum. By contrast, hdm2 with a hydrophobic C-terminus forms a compact conformation and is recognized by the clone A RNA. A single mutation in mdm2 (the mouse form of hdm2), G446S (conserved as glycine 448 in human), completely abolished the specific RNA binding. This is consistent with the structural requirement for RNA binding. The effects of metal binding on the RNA binding properties of hdm2 were also investigated. All evidence suggests that metal binding is not absolutely necessary for specific RNA recognition. This is somewhat surprising considering the numerous zinc finger proteins that requires zinc(II) for proper folding and function.

The RING finger domains of human, mouse, and *Xenopus* hdm2 are highly homologous (Figure 1) (*19*, *41*). Therefore, it is likely to have some important biological functions. While specific RNA recognition did not seem to be affected by metal binding, metal binding and metal-induced folding may be necessary for other activities, for example, protein−protein interaction. Recent studies indicate that hdm2 overexpression induces the destabilization of p53, apparently through a proteasome-dependent pathway that also requires hdm2's export function from the nucleus (*16*−*18*). Although binding of hdm2 to p53 occurs within its N-terminal domain, binding of hdm2 to p53 alone is not sufficient for the degradation of p53. Rather, full-length hdm2 is required. Therefore, the RING finger domain of hdm2 might be necessary for interaction with the import and export machinery and/or for recruiting proteasome components. The biological significance of the presence of the RING finger domain capable of sequential binding to two metal ions in hdm2 remains to be determined.

In summary, the C-terminal domain of hdm2 was found to bind two molecules of zinc(II) in an interleaved fashion similar to the BRCA1 RING finger domain. The binding residues consist entirely of cysteines and one histidine and do not include the threonine for cysteine variation as proposed (*6*). The hdm2 protein exists in a compact conformation in the presence of metal, although no regular structural elements could be identified. It seems that the RNA binding requires a compact conformation of hdm2 with the hydrophobic C-terminus present but does not require metal binding.

ACKNOWLEDGMENT

We are indebted to Dr. B. Elenbaas for helpful discussions. We also like to thank Prof. J. Carey for CD spectrometer time.

REFERENCES

1. Borden, K. L. B., and Freemont, P. S. (1996) *Curr. Opin. Struct. Biol. 6*, 395−401.
2. Freemont, P. S. (1993) *Ann. N.Y. Acad. Sci. 684*, 174−192.
3. Saurin, A. J., Borden, K. L. B., Boddy, M. N., and Freemont, P. S. (1996) *Trends Biochem. Sci. 21*, 208−214.
4. Roehm, P. C., and Berg, J. M. (1997) *Biochemistry 36*, 10240−10245.
5. Miki, Y., Swensen, J., Shattuck-Eisdens, D., Futreal, P. A., Harshman, K., Tavtigian, S., Liu, Q., Cochran, C., and Bennet, L. M. (1994) *Science 254*, 1371−1374.
6. Boddy, M. N., and Freemont, P. S. (1994) *Trends Biochem. Sci. 19*, 198−199.
7. Cordon-Cardo, C., Latres, E., Drobnjak, M., Oliva, M. R., Pollack, D., Woodruff, J. M., Marechal, V., Chen, J., Brennan, M. F., and Levine, A. J. (1994) *Cancer Res. 54*, 794−799.
8. Ladanyi, M., Cha, C., Lewis, R., Jhanwar, S. C., Huvos, A. G., and Healy, J. H. (1993) *Cancer Res. 53*, 16−18.
9. Leach, F. S., Tokino, T., Meltzer, P., Burrel, M., Oliner, J. D., Smith, S., Hill, D. E., Sidransky, D., Kinzler, K. W., and Volgelstein, B. (1993) *Cancer Res. 53*, 2231−2234.
10. Oliner, J. D., Kinzler, K. W., Meltzer, P. S., George, D. L., and Volgelstein, B. (1992) *Nature 358*, 80−83.
11. Reifenberger, G., Liu, L., Ichimura, K., Schmidt, E. E., and Collins, V. P. (1993) *Cancer Res. 53*, 2736−2739.
12. Momand, J., Zambetti, G. P., Olson, D. C., George, D., and Levine, A. J. (1992) *Cell 69*, 1237−1240.
13. Chen, J., Marechal, V., and Levine, A. J. (1993) *Mol. Cell. Biol. 13*, 4107−4114.
14. Freedman, D. A., Epstein, C. B., Roth, J. C., and Levine, A. J. (1997) *Mol. Med. 3*, 248−259.
15. Kussie, P. H., Gorina, S., Marechal, V., Elenbaas, B., Moreau, J., Levine, A. J., and Pavletich, N. P. (1996) *Science 274*, 948−953.
16. Haupt, Y., Maya, R., Kazaz, A., and Oren, M. (1997) *Nature 387*, 296−299.
17. Kubbutat, M. H., Jones, S. N., and Vousden, K. H. (1997) *Nature 387*, 299−303.
18. Roth, J., Dobbelstein, M., Freedman, D. A., Shenk, T., and Levine, A. J. (1998) *EMBO J. 17*, 554−564.
19. Elenbaas, B., Dobbelstein, M., Roth, J., Shenk, T., and Levine, A. J. (1996) *Mol. Med. 2*, 439−451.
20. Burd, C. G., and Dreyfuss, G. (1994) *Science 265*, 615−621.
21. Gill, S. C., and von Hippel, P. H. (1989) *Anal. Biochem. 182*, 319−326.
22. Ellman, G. L. (1959) *Arch. Biochem. Biophys. 82*, 70−77.
23. Riddles, P. W., Blakely, R. L., and Zerner, B. (1979) *Anal. Biochem. 94*, 75−81.
24. Hillel, Z., and Wu, F. Y.-H. (1976) *Biochemistry 15*, 2105−2113.
25. Stryer, L. (1978) *Annu. Rev. Biochem. 47*, 819−846.
26. White, C. E., Ho, M., and Weimer, E. Q. (1960) *Anal. Chem. 32*, 438−440.
27. Melhuish, W. H. (1962) *J. Opt. Soc. Am. 52*, 1256−1258.
28. Chen, R. F. (1967) *Anal. Lett. 1*, 35−42.
29. Longworth, J. W. (1983) *NATO ASI Ser., Ser. A69*, 651−686.
30. Deng, W. P., and Nickloff, J. A. (1992) *Anal. Biochem. 200*, 81−88.
31. Ho, S. N., Hunt, H. D., Horton, R. M., Pullen, J. K., and Pease, L. R. (1989) *Gene 77*, 51−59.
32. Wiskowski, R. T., Hattman, S., Newman, L., Clark, K., Tierney, D. L., Penner-Hahn, J., and McLendon, G. L. (1995) *J. Mol. Biol. 247*, 753−764.
33. Fitzgerald, D. W., and Coleman, J. E. (1991) *Biochemistry* 5195−5201.
34. Krizek, B. A., Merkle, D. L., and Berg, J. M. (1993) *Inorg. Chem. 32*, 937−940.

35. Michael, S. F., Kilfoil, V. J., Schmidt, M. H., Amann, B. T., and Berg, J. M. (1992) *Proc. Natl. Acad. Sci. U.S.A. 89*, 4796−4800.
36. Lovering, R., Hanson, I. M., Borden, K. L., Martin, S., O'Reilly, N. J., Evan, G. I., Rahman, D., Pappin, D. J. C., Trowsdale, J., and Freemont, P. S. (1993) *Proc. Natl. Acad. Sci. U.S.A. 90*, 2112−2116.
37. Teale, F. W. J., and Weber, G. (1957) *Biochem. J. 65*, 476−482.
38. Vallee, B. L., and Auld, D. S. (1990) *Biochemistry 29*, 5647−5659.
39. Borden, M. N., Boddy, M. N., Lally, J., O'Reilly, N. J., Martin, S., Howe, K., Solomon, E., and Freemont, P. S. (1995) *EMBO J. 14*, 1532−1541.
40. Barlow, P. N., Luisi, B., Milner, A., Elliot, M., and Everett, R. (1994) *J. Mol. Biol. 237*, 201−211.
41. Marechal, V., Elenbaas, B., Taneyhill, L., Piette, J., Mechali, M., Nicolas, J.-C., Levine, A. J., and Moreau, J. (1997) *Oncogene 14*, 1427−1433.

BI980596R